*Pramana – J. Phys.* (2017) 88: 72
DOI 10.1007/s12043-017-1378-z



# A new source of radiation in single-bubble sonoluminescence

MORTEZA PISHBINI[1,*] and RASOUL SADIGHI-BONABI[2]

[1]Department of Physics, Payame Noor University, P.O. Box 19395-3697, Tehran, Iran
[2]Department of Physics, Sharif University of Technology, P.O. Box 11365-91, Tehran, Iran
*Corresponding author. E-mail: morteza.pishbini@gmail.com

MS received 23 April 2016; revised 14 November 2016; accepted 16 December 2016; published online 28 March 2017

**Abstract.** An unsolved challenge of sonoluminescence phenomenon is the mechanism of light emission at the moment of collapse. In this article, by considering single-bubble sonoluminescence and based on the hydrochemical model and thermal bremsstrahlung approach, for the first time two different origins of light have numerically been studied to describe the Ar bubble radiation in water at the moment of collapse: (a) radiation from the Ar gas inside the bubble and (b) radiation from the thin layer of the surrounding fluid. The results indicate that, contrary to the previous studies, the radiation from the water shell is dominant, and it is about one order of magnitude stronger than the radiation from the gas inside the bubble. This result can decrease the difference between the theoretical results and the previous experimental data. In addition, based on the role of acoustic pressure amplitude on the characteristics of single-bubble sonoluminescence, various parameters such as degree of ionization, gas pressure, temperature and power were calculated. The results are in excellent agreement with the reported experimental measurements.

**Keywords.** Sonoluminescence; hydrochemical simulation; bremsstrahlung mechanism.

**PACS Nos 82.20.−w; 34.10.+x; 34.50.Ez**

## 1. Introduction

Since the production of periodic picosecond light pulses from the sound waves concentrated inside a collapsing microbubble by Gaitan *et al*, great progress has been made in the field of sonoluminescence (SL) phenomenon [1,2]. Various parameters of the collapsing bubble, such as radius, pressure, temperature and power, are investigated both theoretically [3] and experimentally [4]. It is reported that these parameters are very sensitive to ambient pressure [4,5], ambient temperature [4,6,7], noble gas content [8] and host liquid concentration [9,10]. However, this tiny bubble actually became a very useful microdevice to test the features of various gases, especially rare gases, in extremely high temperatures which cannot be achieved with existing heaters and ovens [8]. Temperatures of several hundreds of thousands degrees kelvin in single-bubble sonoluminescence (SBSL) motivated researchers to use this system for sonofusion [11,12]. The major challenge in SL phenomenon for theoretical and experimental researchers is the mechanism of light emission at the time of collapse. In spite of introducing various mechanisms to explain light emission, such as blackbody radiation, collision induced by the gas molecules and thermal bremsstrahlung radiation, a complete model that describes all experimental achievements is never presented. However, each of these mechanisms explains this phenomenon with some differences in some temperature ranges. Most of the recent works are based on the thermal bremsstrahlung approach [3,13]. However, in spite of fairly close values of measured intensities in some temperatures, the calculated light intensities are about an order of magnitude less than the values reported experimentally [10,14–16].

In this work, a new source of radiation is considered in the host liquid, and a numerical study of the SBSL emission from an Ar bubble in water and its relation to the acoustic pressure amplitude is done. We consider two origins of light for SBSL at the time of collapse: radiation from the Ar gas inside the bubble and radiation from the spherical thin layer of liquid around the bubble [17]. Therefore, for the first time, a comparison is made between the SL power from the bubble

and the water shell around it. Furthermore, it is noticed that the bubble characteristics such as radius, temperature, pressure, degree of ionization and SL radiation are strongly pressure-dependent. This new model and related valuable discoveries are discussed below in detail.

## 2. Model

For considering the interior evolution of the bubble under SL conditions, several models, such as quasiadiabatic compression model [18], molecular dynamics (MD) simulation [19,20] etc. are available. However, each of these models has its own disadvantages. The quasiadiabatic model is very simple and describes the interior evolution of the bubble which is adiabatic at the time of collapse, due to the very short collapsing time, and isothermal in the rest of the cycle. However, in this model, many important parameters of the bubble and the host liquid, such as chemical reactions, are ignored. MD simulation is time consuming and only applicable to systems that are smaller than their corresponding ones in reality. The theoretical model used in the present study is the hydrochemical model. This model, offered for the first time by Yasui [21], includes many properties and complexities such as diffusion, viscosity, chemical reactions, water vapour condensation and evaporation, heat exchange between the noble gas and the surrounding liquid and ionization of atoms and molecules [22].

### 2.1 *Bubble nonlinear radial dynamics*

In this phenomenon, the spherical boundary is the wall of the moving bubble and its nonlinear radial dynamics can be described by the Rayleigh–Plesset equation [23]

$$\left(1-\frac{\dot{R}}{C_{\mathrm{l}}}\right)R\ddot{R}+\frac{3}{2}\left(1-\frac{\dot{R}}{3C_{\mathrm{l}}}\right)\dot{R}^2 = \left(1+\frac{\dot{R}}{C_{\mathrm{l}}}\right)\frac{1}{\rho}(P_{\mathrm{g}}-P_{\mathrm{a}}-P_0) + \frac{\dot{R}}{\rho C_{\mathrm{l}}}P_{\mathrm{g}}-4\mu\frac{\dot{R}}{R}-\frac{2\sigma}{\rho R}. \quad (1)$$

In the hydrochemical model, liquid pressure ($P_{\mathrm{l}}$) and the pressure of Ar noble gas inside the SL bubble ($P_{\mathrm{g}}$) are expressed as

$$P_{\mathrm{l}} = P_{\mathrm{g}} - 4\frac{\mu\dot{R}}{R} - 2\frac{\sigma}{R},$$
$$P_{\mathrm{g}}(t) = \frac{N_{\mathrm{tot}}(t)\,k_{\mathrm{B}}T_{\mathrm{g}}}{V - N_{\mathrm{tot}}(t)B} \quad (2)$$

In these equations, $R$ is the bubble radius, $\dot{R}$ and $\ddot{R}$ are its time derivatives. $C_{\mathrm{l}}$, $\rho$, $\mu$, $\sigma$ are the speed of sound in the liquid, density of the liquid on the liquid side of the bubble wall, viscosity coefficient of the liquid, and surface tension coefficient of the liquid, respectively. $P_0$, $P_{\mathrm{l}}$, $P_{\mathrm{a}}$ and $P_{\mathrm{g}}$ are ambient pressure, liquid pressure, driving acoustic pressure amplitude at the location of the bubble that $P_{\mathrm{a}} = -p_{\mathrm{a}}(\sin\omega t)$ and $\omega$ is the frequency of the acoustic wave and pressure on the gas side of the bubble wall, respectively. $N_{\mathrm{tot}}$, $T_{\mathrm{g}}$, $B$ and $k_{\mathrm{B}}$ are the total number of particles inside the bubble, the temperature of the gas inside the bubble, the hard core parameter ($B = 5.1 \times 10^{-29}$ m$^3$) and the Boltzmann constant, respectively.

### 2.2 *Interior evolutions*

In this model, variation of the temperature of the Ar gas with time is calculated from [10]

$$\dot{T}_{\mathrm{g}}\frac{\partial e_{\mathrm{th},j}}{\partial T_{\mathrm{g}}}N_j = \dot{Q} - P_{\mathrm{g}}\dot{V} - \sum_J e_{\mathrm{th},j}N_j + \dot{E}_{\mathrm{chem}} + \sum h_{w,j}N_j^d, \quad (3)$$

where $T_{\mathrm{g}}$ is the temperature of the Ar gas, $N_j$ denotes the vapour species $j$ inside the bubble and $\dot{N}_j$ indicates the rate of change in vapour species $j$ inside the SL bubble. $h_{w,i} = (1+\frac{f_j}{2})KT_0$ is the molecular enthalpy of the particles of species $j$ at the bubble wall temperature $T_0$, with $f_j$ as its number of translational + rotational degrees of freedom. The quantity $\dot{E}_{\mathrm{chem}}$ indicates the rate of change in the chemical energy of the bubble due to reactions considered in the hydrochemical model. $\dot{Q}$ and $V$ are the rate of heat transfer at the bubble wall and bubble volume, respectively

The quantity $e_{\mathrm{th,j}}$ denotes the thermal energy of the species $j$ and is given by

$$e_{\mathrm{th},j} = \frac{f_j}{2}KT_{\mathrm{g}} + \sum_l \frac{K\Theta_{j,l}}{\exp(\Theta_{j,l}/T_{\mathrm{g}})-1} \quad (4)$$

with $\Theta_{j,l}$ as the various characteristic vibrational temperatures of the particle species $j$. Complete details of eq. (3) can be observed in refs [22,24] and is not repeated here. By numerical solution of the resulting set of equations in the hydrochemical model, we can obtain radial variation and thermodynamic evolution inside the bubble.

### 2.3 *Thermal bremsstrahlung radiation*

Based on the very hot environment at the moment of light emission, one can assume an ionized state in the bubble at the time of collapse. We assume that the

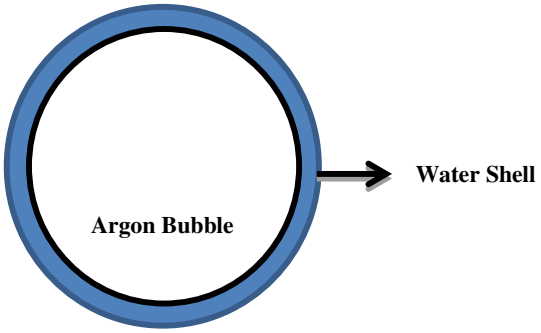


**Figure 1.** Two origins of light in a sonoluminescencing bubble.

temperature gradient in the surrounding fluid is zero except at the spherical thin layer around the bubble (figure 1) and that due to the diffusion of free electrons at the moment of collapse from the hot bubble to the fluid, this part of the fluid can be considered to be in an ionized state [17]. Due to the existence of free electrons and ions inside and outside the bubble, the thermal bremsstrahlung model is used to interpret the radiated intensity from two origins [3]. To obtain bremsstrahlung power of the water shell, one needs to calculate $\sigma_{bf}$, the cross-section of photoionization of water [3]. For $H_2O$ molecule, due to the negligible molar weight of hydrogen in comparison to the oxygen atoms, we assume that the oxygen atom is dominant.

**Table 1.** Different parameters of Ar and water molecules which are used in the simulation.

| | $\chi$ (J) | $\sigma_{fb}$ (m$^2$) | $\sigma_{bf}$ (m$^2$) |
|---|---|---|---|
| Argon | $2.53 \times 10^{-18}$ | $10^{-24}$ | $10^{-20}$ |
| Water | $1.69 \times 10^{-18}$ | $10^{-25}$ | $1.38 \times 10^{-23}$ |

Therefore, we calculate this parameter by an equation from ref. [25], the cross-section of photoionization for oxygen is calculated to be about $1.38 \times 10^{-23}$ m$^2$. To obtain the rate of recombination ($r_r$) which forms the main part of the light intensity, one needs to have $\sigma_{fb}$, the cross-section of the radiative recombination. The specific values of $\sigma_{fb}$ are not reported for oxygen, but their values probably are of the same order as that of hydrogen or even larger [26]. Therefore, we assume that $\sigma_{fb}$ is about $10^{-25}$ m$^2$ for the oxygen atoms. The number of free electrons ($n_e$) in a spherical thin layer of water can be calculated by the Saha equation [3,27]. To obtain $n_e$, we should have the ionization potential of the water atoms, that is $\chi_W = 10.56$ eV $= 1.69 \times 10^{-18}$ J. Different parameters of Ar and water molecules are listed in table 1.

## 3. Numerical simulation and results

In this section, the results of our numerical calculations for an SL bubble in water containing Ar as the doped noble gas with relative gas concentration of $c_\infty/c_0 = 0.004$, by using the hydrochemical simulation code with the Runge–Kutta algorithm, are given. The frequency of the driving pressure and the ambient pressure for all calculations were set at 38 kHz and 1.0 atm, respectively. In order to have a stable SL bubble, for long time oscillations in water, three major instabilities, i.e., shape, diffusion and Bjerknes instabilities are considered [8–28]. These instabilities can be displayed simultaneously in a region of ($R_0$, $P_a$), which is called phase space. By using the phase diagram, we can

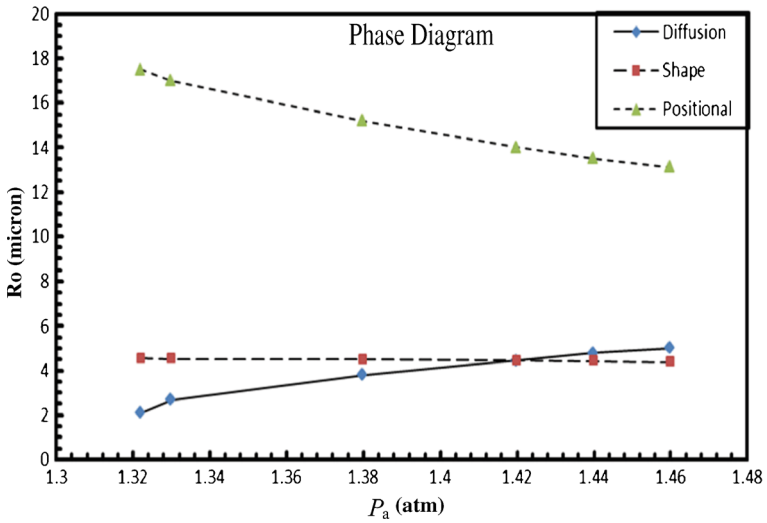


**Figure 2.** Phase diagram for an SL bubble in water containing Ar, with a relative gas concentration of $c_\infty/c_0 = 0.004$.

**Table 2.** The bubble parameters presented at the time of collapse.

| $P_a$ (atm) | $R_0$ ($\mu$m) | $T_{gmax}$ ($K$) | $P_{gmax}$ (atm) | $R_{min}/R_0$ | $R_{max}/R_0$ | $R_{max}/R_{min}$ |
|---|---|---|---|---|---|---|
| 1.33 | 2.67 | 24491 | 60347 | 0.155 | 9.461 | 61.04 |
| 1.38 | 3.80 | 28903 | 71603 | 0.152 | 9.012 | 59.29 |
| 1.42 | 4.45 | 31205 | 76719 | 0.151 | 8.85 | 58.61 |

theoretically obtain the permissible range of ambient radius and acoustic pressure amplitude for stable SBSL. The resulting equilibrium curves for an Ar bubble in water at room temperature are shown in figure 2. In this diagram, the lines connecting points help to guide the eye. As shown in figure 2, due to the low viscosity of water, the phase parameters of the bubble oscillations are determined by the diffusion and shape instability curves. In addition, the ultimate driving pressure for a stable SL is restricted by the shape instability curve. Accordingly, in the area under and along the diffusion curve with ultimate pressure 1.42 atm, the bubble has three major stabilities. Furthermore, the maximum SL emission is obtained at the point where the diffusion curve crosses the shape instability curve because pressure and the initial radius are maximum. It should be noted that, according to the phase diagram, the SL bubble with initial conditions ($R_0$, $P_a$) on the diffusion instability curve with positive slope is diffusively stable.

According to the phase diagram, to ensure the stability of the bubble by changing the pressure amplitude, we had to change the initial radius of the bubble ($R_0$) as shown in table 2.

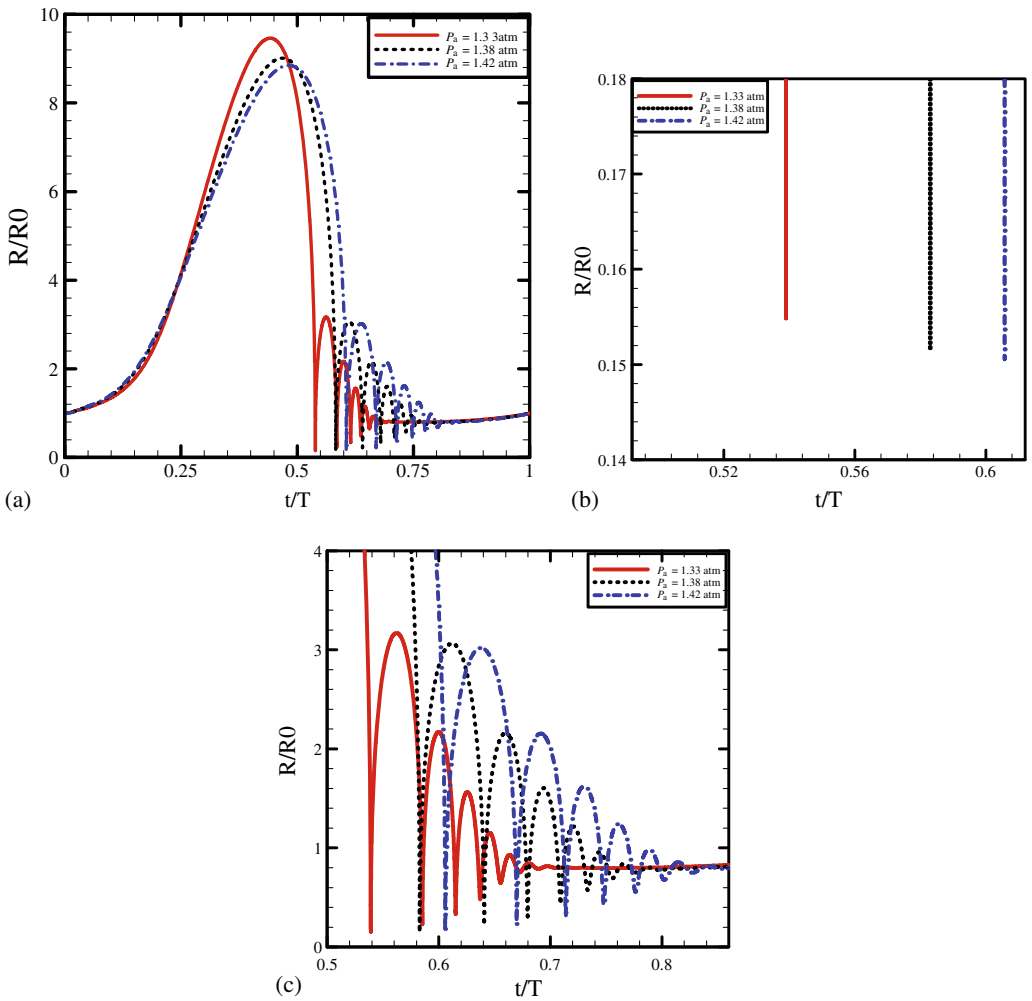


**Figure 3.** Time evolution of the (**a**) normalized bubble radius, (**b**) minimum radius and (**c**) after bounces in three different acoustic pressure amplitudes, at ambient temperature $T_0 = 293.15$ K. The total time of one acoustical cycle is $T$.

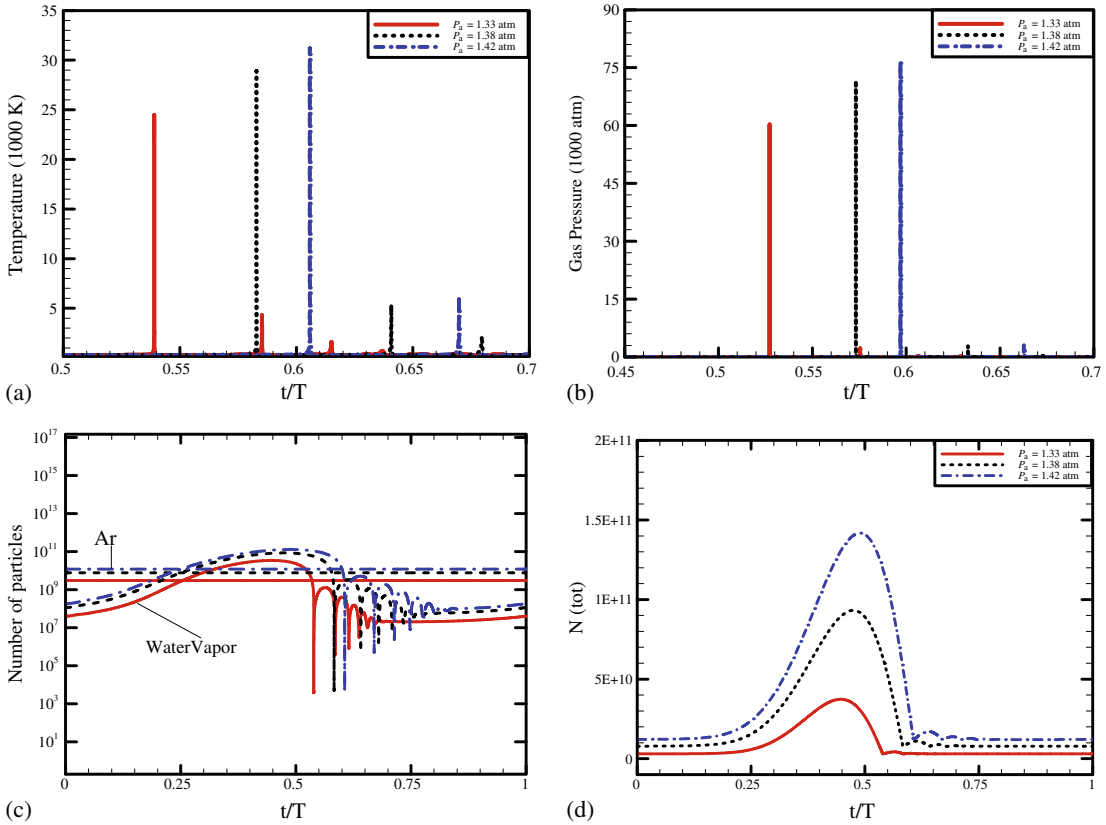


**Figure 4.** Bubble characteristics as a function of time in three different acoustic pressure amplitudes: (**a**) interior temperature of the bubble, (**b**) gas pressure inside the bubble, (**c**) the number of Ar and $H_2O$ particles and (**d**) the total number of particles inside the bubble.

The time evolution of the radius of an oscillating bubble in one cycle under different acoustic pressures, is shown in figure 3. The axis of the bubble radius is normalized to $R_0$, that is the initial radius of the bubble. It is seen that, the strength of collapse varies for various acoustic pressures and this is observed in the difference between the expansion ratio, ER $= R_{\max}/R_0$, and the amplitude of mutations that occur after the moment of collapse in different acoustic pressures. Furthermore, figure 3 shows that, increase in the amplitude of the acoustic pressure increases the collapse time and decreases the minimum and maximum radii of the bubble.

Figure 4 shows the bubble characteristics as a function of time, by using the hydrochemical model for

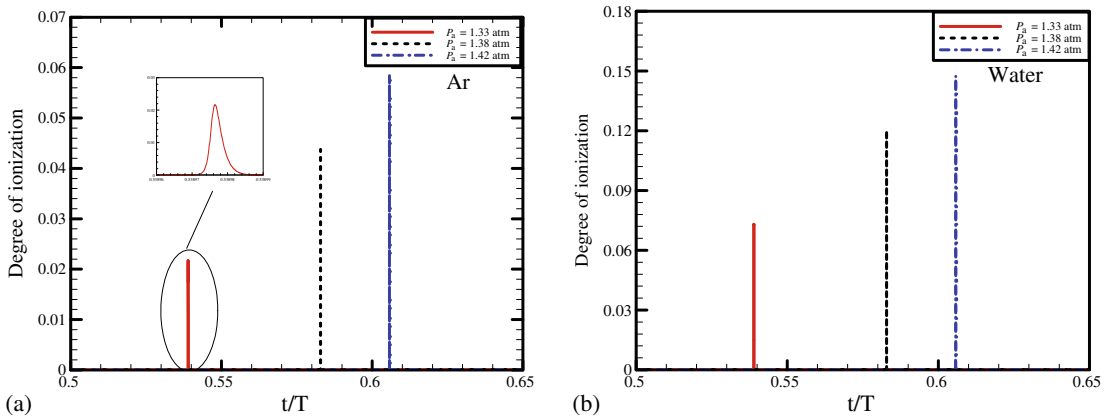


**Figure 5.** Time variation of the degree of ionization for (**a**) Ar molecules inside the bubble and (**b**) water molecules inside the water shell, in three different acoustic pressure amplitudes.

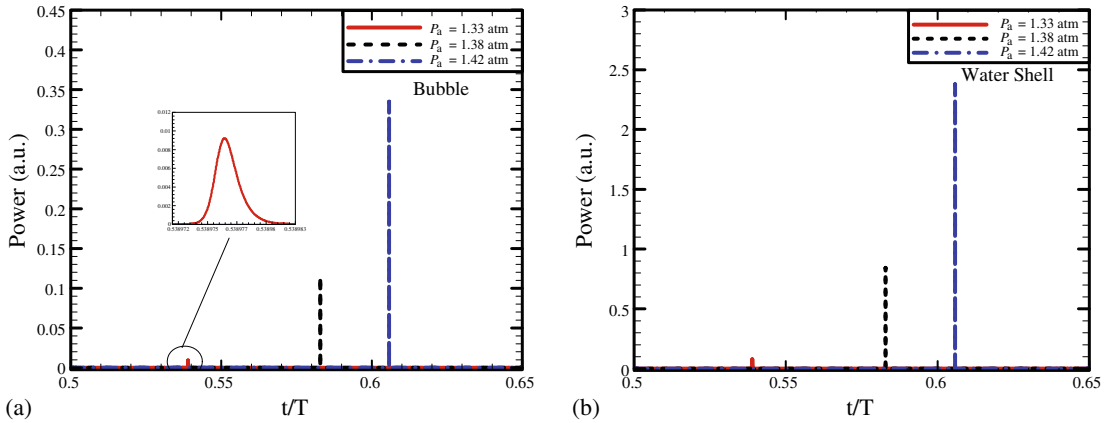


**Figure 6.** The SL power from (**a**) bubble and (**b**) water shell for three different acoustic pressure amplitudes at $T_0 = 293.15$ K.

evolution of the gas inside the bubble. It can be seen from figures 4a and 4b that the increment in pressure amplitude results in a time delay in the time-dependent variation of the temperature and pressure of the gas inside the bubble. Furthermore, because of the larger value of Ar and ambient radius, temperature and pressure peaks increase as the amplitude of pressure increase.

It is also noticed that, mutations that occur after the moment of collapse are more distinguished when the acoustic pressure increases. In figures 4c and 4d the number of water vapour molecules, Ar molecules

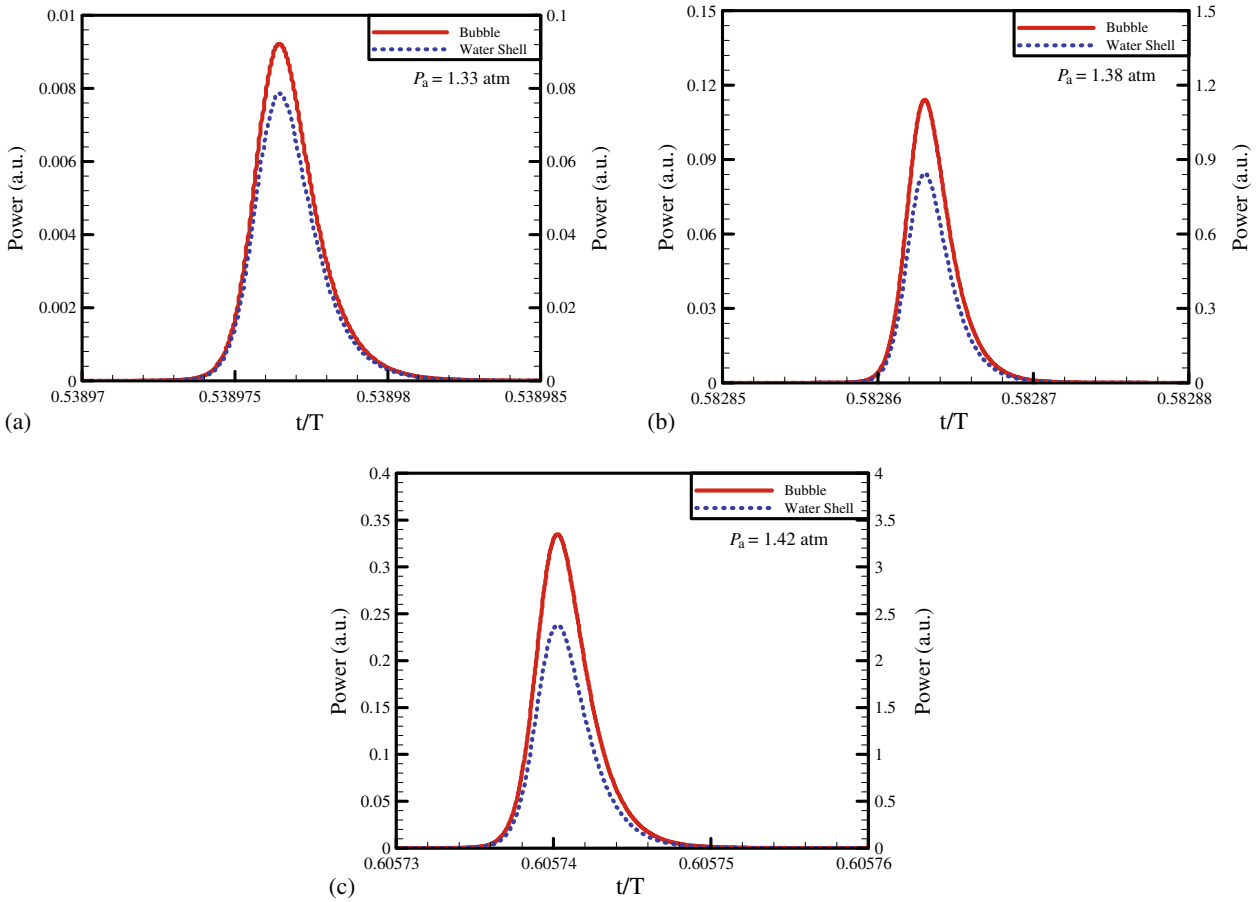


**Figure 7.** Comparison of SL power, from bubble (left axis) and water shell (right axis) for three acoustic pressure amplitudes: (**a**) 1.33 atm, (**b**) 1.38 atm and (**c**) 1.42 atm.

and the total number of particles inside the SBSL for different acoustic pressure amplitudes are indicated. It can be seen that, Ar and water vapour molecules and consequently the total number of particles decrease as the acoustic pressure amplitude is reduced. In addition, we know that the number of endothermic reactions inside the bubble at the moment of collapse is determined by the amount of water vapour molecules. The calculation shows that there is a reduction in the number of water vapour molecules at the moment of collapse with a decrease in the acoustic pressure amplitude (figure 4c). Details of our calculations and values of the bubble characteristics are shown in table 2.

In the following, for an Ar bubble and water shell, we investigate how the degree of ionization varies with time (figure 5). To calculate the degree of ionization at any time, Saha equation is used [27]. At the time of collapse, due to high temperature and pressure, the Ar and water vapour molecules inside the bubble and water molecules outside the bubble in the spherical water shell will be ionized. As shown in figure 4c, the number of Ar molecules at the time of collapse is much more than the number of water vapour molecules inside the bubble, and so we consider only the degree of ionization of Ar molecules. The ionization energy of the Ar molecules is much larger than that of the water molecules (see table 1) and so the degree of ionization in the water shell must be larger.

In this section, the power of the emitted light in one cycle by three major mechanisms, i.e., radiative recombination, electron–atom bremsstrahlung and electron–ion bremsstrahlung, is calculated. Figure 6 shows SL power from the gas inside the bubble and the spherical water shell, for different acoustic pressure amplitudes. It is noticed that, by increasing the acoustic pressure amplitude, the power increases for both the gas inside the bubble and the spherical water shell. In addition, the SL power from the water shell is remarkably greater than the SL power from the gas inside the bubble at the moment of collapse. It can be seen that, the pressure increment results in a time delay in the time of collapse. This is verified in an earlier experimental work [16].

In figure 7, the SL power from the gas inside the bubble and the spherical water shell, in different acoustic pressures, is compared. The left and right vertical axes are related to the gas bubble and the water shell power, respectively. As shown in figure 7, and in contrast to the earlier reports of SBSL, the SL power from the spherical water shell in three acoustic pressure amplitudes is about one order of magnitude more than the power from the gas inside the bubble and consequently it is the dominant radiation in the SL phenomenon.

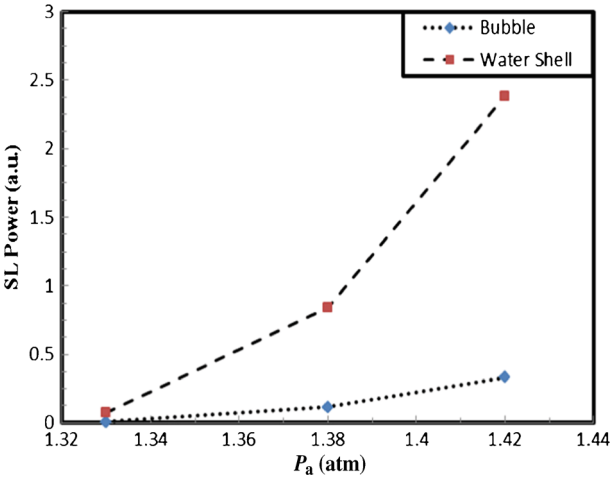


**Figure 8.** The results of simulation for SL power from bubble and water shell in three acoustic pressure amplitudes.

This can be due to the existence of more free electrons, because of smaller ionization potential of water. According to the Saha equation, the smaller ionization potential of water compared to Ar atoms leads to a greater degree of ionization of water (see figure 5). Therefore, the greater SL power from the water shell is justified. In addition, as shown in figure 7, it is clear that the increment in pressure amplitude results in a time delay in the SL power from two sources of light.

Following the strong dependence of the SL power on the acoustic pressure amplitude, the simulation results for SL power in three acoustic pressure amplitudes for gas bubble and water shell is shown in figure 8. It is very interesting to see that, the SL power is strongly pressure-dependent where the values at lower pressure are about three orders of magnitude lesser than the intensity at the higher pressures. In this diagram the lines only indicate the path.

## 4. Conclusion

In the present work, a new source of light to describe the emission from a SBSL at the moment of collapse is introduced. In addition, the Ar bubble parameters and its evolution in water, for three acoustic pressure amplitudes, are calculated. By assuming electron diffusion during the bubble collapse, we suppose that both the spherical thin layer of the surrounded fluid and the gas inside the bubble radiate light pulses. By using the bremsstrahlung model, it is proved that the SL power from the spherical water shell is about one order of magnitude stronger than the one from the Ar gas inside the bubble and it is closer to the previous

experimental values. Due to the existence of more free electrons, because of smaller ionization potential of the water shell and high compression of ionized particles in this part, the radiation from the water shell will be brighter. As a consequence, contrary to the earlier reports, the power from the gas inside the bubble is negligible compared to that due to the water shell and the radiation from the water shell formed is dominant in the bremsstrahlung model.

## References


[1] D F Gaitan, L A Crum, C C Church and R A Roy, *J. Acoust. Soc. Am.* **91**, 3166 (1992)

[2] B P Barber, R A Hiller, R Lofstedt, S J Putterman and K R Weninger, *Phys. Rep.* **281**, 65 (1997)

[3] K Yasui, *Phys. Rev. E* **60**, 1754 (1999)

[4] G E Vazquez and S J Putterman, *Phys. Rev. Lett.* **85**, 3037 (2000)

[5] M Dan, J D N Cheeke and L Kondic, *Ultrasonics* **38**, 566 (2000)

[6] K Yasui, *Phys. Rev. E* **64**, 016310 (2001)

[7] S Hilgenfeldt, D Lohse and W C Moss, *Phys. Rev. Lett.* **80**, 1332 (1998)

[8] M P Brenner, S Hilgenfeldt and D Lohse, *Rev. Mod. Phys.* **74**, 425 (2002)

[9] A Troia, D M Ripaa and R Spagnolo, *Ultrason. Sonochem.* **13**, 278 (2006)

[10] A Moshaii, K Imani and M Silatani, *Phys. Rev. E* **80**, 046325 (2009)

[11] R P Taleyarkhan, C D West, J S Cho, R T Lahey, R I Nigmatulin and R C Block, *Phys. Rev. E* **69**, 036109 (2004)

[12] N Zoghi-Foumani and R Sadighi-Bonabi, *Int. J. Hydrogen Energy* **39**, 11328 (2014)

[13] F Bemani and R Sadighi-Bonabi, *Phys. Rev. E* **87**, 013004 (2013)

[14] S Hilgenfeldt, S Grossmann and D Lohse, *Nature* **398**, 402 (1999)

[15] D F Gaitan, A A Atchley, S D Lewia, J T Carlson and X K Maruyama, *Phys. Rev. E* **54**, 525 (1996)

[16] Y Didenko, W McNamara and S K Suslick, *Nature* **407**, 877 (2000)

[17] V A Borissenok, *Phys. Lett. A* **372**, 3496 (2008)

[18] H Kwak and J H Na, *Phys. Rev. Lett.* **77**, 4454 (1996)

[19] S J Ruuth, S Putterman and B Merriman, *Phys. Rev. E* **66**, 036310 (2002)

[20] M Matsumoto, K Miyamoto, K Ohguchi and T Kinjo, *Prog. Theor. Phys. Suppl.* **138**, 728 (2000)

[21] K Yasui, *Phys. Rev. E* **56**, 6750 (1997)

[22] A Moshaii and R Sadighi-Bonabi, *Phys. Rev. E* **70**, 016304 (2004)

[23] J B Keller and M J Miksis, *J. Acoust. Soc. Am.* **68**, 628 (1980)

[24] A Moshaii, R Rezaei-Nasirabad, K H Imani, M Silatani and R Sadighi-Bonabi, *Phys. Lett. A* **372**, 1283 (2008)

[25] S Eliezer, *The interaction of high-power lasers with plasmas* (IOP Publishing Ltd, London, 2002)

[26] S C Brown, *Basic data of plasma physics* (AIP, New York, 1994)

[27] Y B Zeldovich and Y P Raizer, *Physics of shock waves and high-temperature hydrodynamic* (Academic Press, New York, 1966)

[28] X Lu, A Prosperetti, R Toegel and D Lohse, *Phys. Rev. E* **67**, 056310 (2003)